 © 1986 The Chemical Society of Japan Bull. Chem. Soc. Jpn., 59, 3431—3437 (1986)

High-Temperature Reaction of NH_3-N_2O System in Shock Waves

Nobuyuki Fujii, Syuji Uchida, Hisaaki Sato, Shiro Fujimoto† and Hajime Miyama*

Department of Materials Science and Technology, The Technological University of Nagaoka, Kamitomioka, Nagaoka 940-21

(Received May 21, 1986)

The high-temperature reaction of NH_3 with N_2O in shock waves was investigated by measuring ultaviolet absoption of NH_3 and OH, and infrared emission of N_2O, in the temperature range of 1700—2300 K on the mixture of NH_3-N_2O diluted with large amount of argon. A comparison of the observed decays of NH_3 and N_2O and the formation of OH with those obtained by computer simulation behind the incident shock wave was carried out. From the comparison, the rate constants of the following elementary reactions were determined: $NH_3+O\rightarrow NH_2+OH[k_4=10^{12.5}\exp(-25.5\ \mathrm{kJ}/RT)\ \mathrm{cm^3\ mol^{-1}\ s^{-1}}]$; $NH_3+OH\rightarrow NH_2+H_2O[k_5=10^{12.5}\exp(-8.4\ \mathrm{kJ}/RT)\ \mathrm{cm^3\ mol^{-1}\ s^{-1}}]$.

The high-temperature oxidation of NH_3 has been studied by many researchers,[1-4] and it was reported that NH_2 radicals play important roles.[1] Among the formation reaction of NH_2, the most important reactions in the initial stage of the reaction, $NH_3+O\rightarrow NH_2+OH$ and $NH_3+OH\rightarrow NH_2+H_2O$ have been investingted by several reserchers and their rate constants have been recommended.[5,6] However, larger values of the rate constants have also been reported.[4,7-9]

The objective of the present work is to examine the above two rate constants precisely by measuring spectroscopically the concentrations of NH_3, N_2O, and OH in the high-temperature reaction of NH_3-N_2O system in shock waves. Since the high temperature dissociation of N_2O is the initiation reaction of above reaction system and its rate constants have been determined exactly,[8,10,11] the decomposition of N_2O was studied in the incident shock waves at first. Simulatin of the reaction was carried out and the results were compared with the experiments. After confirming the accuracy of this experimental technique by the comparison, reaction of NH_3-N_2O was studied in the incident shock waves.

Experimental

The shock tube used in this study is made of stainless steel tubing of 46 mm internal diameter, consisting of a test section of 3.6 m long, a high-pressure section of 2 m long and a dump tank located at the end of the test section. The shock tube had a leak rate less than 5×10^{-4} Torr min^{-1} (1 Torr=133.322 Pa) and was evacuated to less than 2×10^{-4} Torr before each experiment. Polyester diaphragms were pressure burst using H_2 driver gas. The incident shock wave velocity was measured by four piezo-electric gauges located at intervals of 200 mm and a time counter, and the shock parameters were calculated from the shock velocity. An observation section is installed at 3.1 m down stream from the diaphragm. The time history of NH_3 was monitored by measuring the ultraviolet absorption of NH_3 at 200 nm by using an optical system consisting of a D_2 lamp, a monochromator, and a photomultiplier. N_2O time history was monitored by the infrared emission of N_2O at 4.52 μm with an InSb detector through an interference filter (half width: 0.18 μm). Also at the same location, the pressure profile was measured by a piezoelectric gauge. On the other hand, simultaneously with measurement of NH_3, the formation of OH radical was observed by resonant absorption at 306 nm by using OH lamp powered by a microwave discharge in a flow of H_2O vapor. Calibration of OH absorption was carried out by the exeriment of shock heated H_2-O_2-Ar mixtures. These signals were displayed on a digital storage oscilloscope. Experiments were carried out on mixtures of N_2O (1%) and argon (99%) and of NH_3 (1—2%), N_2O (0.3—1%) and argon (97.6—98.7%). The experimental conditions were; 1700—2300 K and 0.9—2.1 atm as summarized in Table 1.

Results and Discussion

Dissociation of N_2O. High-temperature decom-

Table 1. Experimental Conditions

Mixture	N_2O %	NH_3 %	Ar %	T_{20} K	p_{20} atm
I	1.0	0	99.0	1690—2010	1.89—2.04
II	0.3	1.0	98.7	1690—2310	1.78—2.04
III	1.0	1.0	98.0	2000—2260	2.04—2.14
IV	0.4	2.0	97.6	1860—2290	0.91—1.05
V	1.0	1.0	98.0	1770—2040	1.92—2.14

1 atm=101325 Pa.

† Present address: Department of Chemistry, National Defense Academy, Hashirimizu, Yokosuka 239.

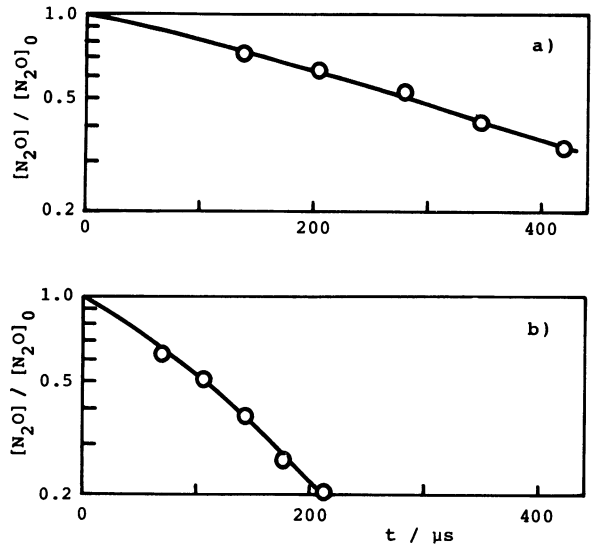

Fig. 1. Examples of the comparison of the experimentally measured N_2O first order decays in mixture I (symbols) with simulated ones (lines). a): $T_0=1855$ K, $p_0=2.01$ atm, b): $T_0=2010$ K, $p_0=1.93$ atm.

position of N_2O has been studied by many researchers[8,10,11] and its reaction scheme is well-established. That is, the following elementary reactions (1)—(3) are important at the inital stage of the reaction;

(1) $N_2O + M \longrightarrow O + N_2 + M$,
(2) $N_2O + O \longrightarrow NO + NO$,
(3) $N_2O + O \longrightarrow N_2 + O_2$.

When the O atoms are in the steady state, the decomposition rate of N_2O is given by the following equation;[8,10]

$$d[N_2O]/dt = -2k_1[N_2O][M], \quad (1)$$

where [M] is the concentration of the third body. Accordingly, the rate constant of the dissociation of N_2O is obtained as follows by integrating Eq. 1;

$$k_1 = (2[M]t)^{-1} \ln([N_2O]_0/[N_2O]), \quad (2)$$

where subscript 0 shows the initial condition.

In the present experiment, the decay profile of N_2O infrared emission intensity measured behind the incident shock wave deviated from the first-order rate law as the reaction proceeded. Examples of the decay of N_2O are shown in Fig. 1. From the initial slope of the emission, the rate constants for the dissociation of N_2O were obtained according to Eq. 2. They are listed with the experimental conditions in Table 2. The Arrhenius plot of k_1 is shown in Fig. 2, together with the values recommended by Baulch et al.,[10] by Just,[11] and by Hanson et al.[8] Agreement between the values obtained in the present experiment and the recommended values are very good. From the plot of Fig. 2, the following Arrhenius expression was obtained;

Table 2. Experimental Results for Mixture I

Run	T_{20} / K	p_{20} / atm	$[M]_{20}$ / mol cm^{-3}	k_1 / cm^3 mol^{-1} s^{-1}
1	1550	2.05	1.61×10^{-5}	3.64×10^{6}
2	1580	1.89	1.44	4.43×10^{6}
3	1680	1.92	1.39	1.38×10^{7}
4	1690	1.93	1.40	1.87×10^{7}
5	1800	2.02	1.38	5.02×10^{7}
6	1855	2.01	1.33	9.58×10^{7}
7	1929	1.89	1.20	1.74×10^{8}
8	2010	1.93	1.18	2.94×10^{8}

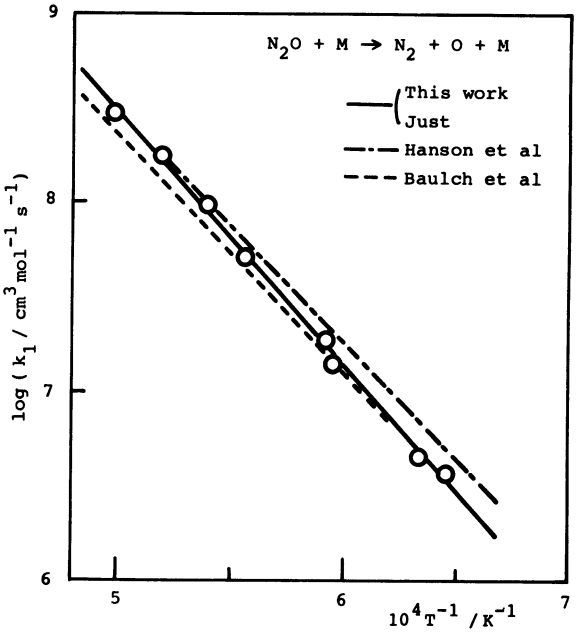

Fig. 2. Arrhenius plots of k_1.

$$k_1 = 10^{15.21}\exp(-257.7\ \text{kJ}/RT)\ \text{cm}^3\ \text{mol}^{-1}\ \text{s}^{-1}.$$

Then, the decay of N_2O was calculated by computer simulation by using elementary reactions (1)—(3) and their reverse reactions. In this calculation, the rate constant of Reaction (1) obtained in this experiment was used and values recently recommended by Hanson et al.[8] for Reactions (2) and (3) were adopted. In this simulation the heat of reaction and the correction for the nonideality of shocked flow caused by the boundary layer behind the incident shock front[12,13] were taken into account. The calculated decay profiles of N_2O agreed with the experiments as shown in Fig. 1. From the results, it was confirmed that the shock tube technique coupled with the above mentioned computer simulation had a good accuracy in the present experiment.

Reaction of NH_3 with N_2O. Reaction mechanism: The reaction of NH_3 with N_2O at high temperatures is initiated by the decomposition of N_2O and the main

Table 3. Reaction Schemes and Rate Parameters[a)]

Reaction	Mechanism A[6)]			Mechanism B[7)]		
	log A	B	E/kJ	log A	B	E/kJ
1. $N_2O + M \rightarrow N_2 + O + M$	15.21		257.7	23.84	−2.5	272.0
2. $N_2O + O \rightarrow NO + NO$	13.84		111.7			
3. $N_2O + O \rightarrow N_2 + O_2$	14.00		117.2			
4. $NH_3 + O \rightarrow NH_2 + OH$	12.49		25.5	13.34		37.2
5. $NH_3 + OH \rightarrow NH_2 + H_2O$	12.50		8.4	13.91		35.2
6. $NH_3 + NH_2 \rightarrow N_2H_3 + H_2$	11.90	0.5	90.4			
7. $N_2H_3 + M \rightarrow NH_2 + NH + M$	12.80		41.8			
8. $NH_2 + O \rightarrow NH + OH$	11.96	0.5	0	14.07	−0.5	0
9. $NH_2 + O \rightarrow HNO + H$				14.82	−0.5	0
10. $NH_2 + OH \rightarrow NH + H_2O$				11.70	0.5	8.3
11. $HNO + M \rightarrow H + NO + M$				16.25		203.7
12. $H + N_2O \rightarrow N_2 + OH$				13.88		63.2
13. $H + NH_3 \rightarrow NH_2 + H_2$				14.30		97.4

a) $k = AT^B\exp(-E/RT)$ in units of $cm^3\,mol^{-1}\,s^{-1}$.

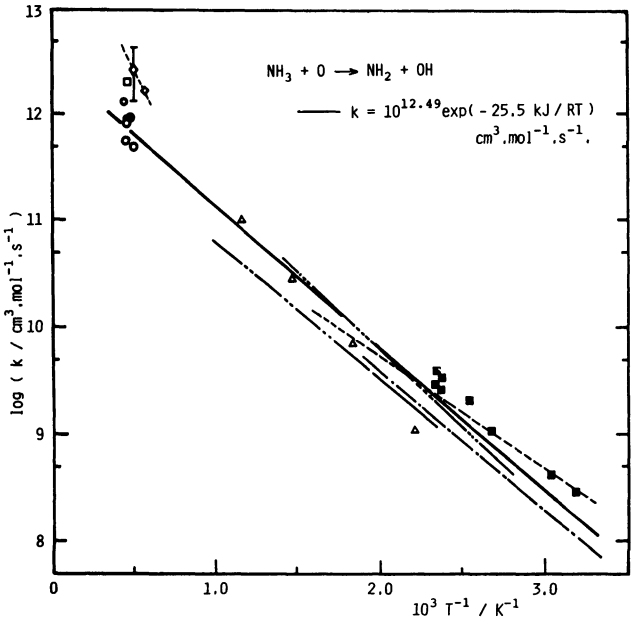

Fig. 3. Arrhenius plots of k_4. Solid line: this work, other lines : from Baulch et al.,[10)] ○: Fujii et al.,[6)] ◇: Salimian et al.,[7)] □: Saito et al.,[14)] ■: Kirchner et al.,[15)] △: Perry.[16)]

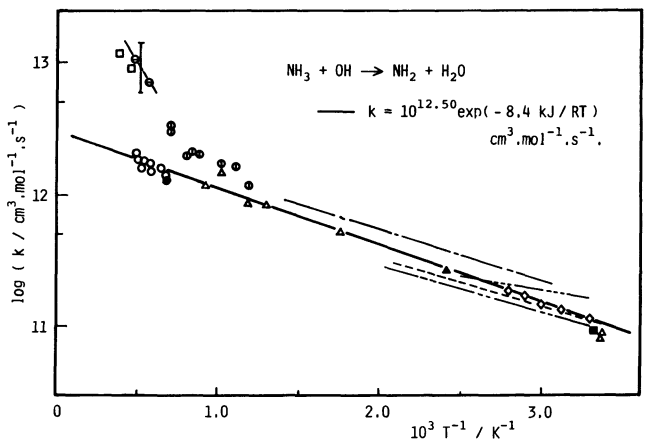

Fig. 4. Arrhenius plots of k_5. Solid line: this work, other lines, ●, △, ▲, ■: from Fujii et al.,[5)] ○: Fujii et al.,[5)] ⊖: Salimian et al.,[7)] □: Zabielski et al.,[9)] ◇: Stephens,[17)] ⓘ: Jeffries et al.[18)]

subsequent reactions are;

(4) $NH_3 + O \longrightarrow NH_2 + OH$, $\Delta H = 28.5\,kJ\,mol^{-1}$,

(5) $NH_3 + OH \longrightarrow NH_2 + H_2O$, $\Delta H = -42.6\,kJ\,mol^{-1}$.

The reaction scheme in the initial stage of this system, presented by Fujii et al. (Mechanism A)[6)] is shown in Table 3. Here, Reactions (1)—(3) are those of the decomposition of N_2O, Reactions (4)—(6) are main reactions for the consumption of NH_3 and Reactions (7) and (8) are the subsequent reactions. Also the scheme reported by Salimian et al. (Mechanism B)[7)] is shown in the table. In this scheme, Reaction (9) is included as the reaction of NH_2 with O, then H atom plays an imporant role for the formation of OH. Also, Salimian el al.[4)] reported the kinetic model including 60 reactions of the N-O, N-H, N-H-O, and O-H system (Mechanism B′). However, the rate constants of many of these reactions were not accurately known and their values were estimated for the simulation.

As for the rate constants k_4 and k_5, Fujii et al.[5)] obtained k_4 by measuring ultraviolet absorption of NH_3 in NH_3-H_2-O_2-Ar mixtures. Also, Fujii et al.[6)] obtained k_5 by measuring ultraviolet absorption of NH_3 and infrared emission of N_2O in NH_3-N_2O-Ar mixtures. On the other hand, Salimian et al.[7)] measured ultraviolet absorption of OH and infrared emission of NH_3 in NH_3-N_2O-Ar mixtures and obtained k_4 and k_5 simultaneously. Zabielski et al.[9)] mea-

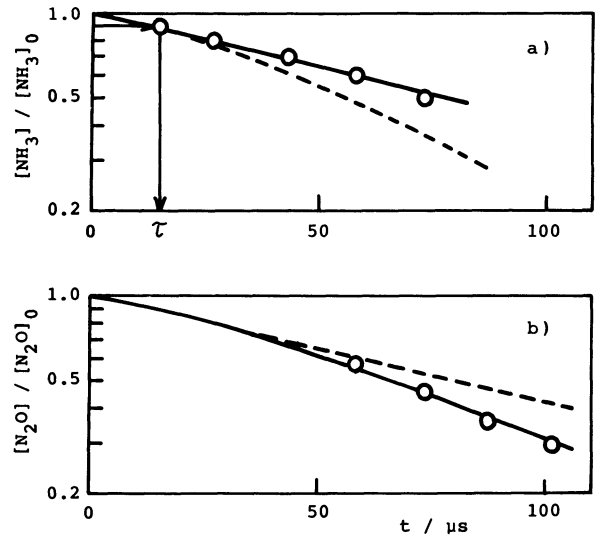

Fig. 5. Examples of the comparison of the experimentally obtained first order decays of NH_3 and N_2O in mixture III (symbols) with simulated ones (lines) T_0=2110 K, p_0=2.13 atm, a): NH_3, b): N_2O.

sured concentration profiles of NH_3, OH, and O in a low-pressure CH_4–O_2–Ar flat flame containing small amounts of NH_3 and obtained k_5 using k_4 given by Salimian et al.[7] The values of k_4 and k_5 by Salimian et al.[7] and k_5 by Zabielski et al.[9] were about 5 times as large as those recommended by Fujii et al.[5,6] Jefferies and Smith[18] measured k_5 over the range 840—1425 K by using an infrared laser pyrolysis technique (10.6 μm) with laser-induced fluolescence detection of OH. The values of k_5 at 1425 K were about 2 times larger than those by Fujii et al.[5] The Arrhenius plots of these rate constants are shown in Figs. 3 and 4, together with the values reported by other researchers. For the experimental data at high and low temperatures, nonlinear-Arrhenius expressions were adopted for k_4 by Salimian et al.[7] and for k_5 by Salimian et al.,[7] Zabielski et al.[9] and Jefferies et al.[18] In order to justify the experimental curved-Arrhenius expression, they calculated the rate constants by the transition state theory using some assumptions. The rate constants of other Reactions (6)—(8) have not yet been measured accurately.

Consumption of NH_3 and N_2O: The concentration of NH_3 decayed almost according to the first order rate law in NH_3–N_2O system. The concentration of N_2O decayed also according to the first-order rate law and the rate of the decay in the equimolar mixture of NH_3 and N_2O was almost similar to that of the decomposition of N_2O. Examples of the first order decays of NH_3 and N_2O are shown in Fig. 5.

In order to examine the contribution of each elementary reaction to the decay rate of NH_3, the sensitivity checks described previously[1] were applied as follows. The decay of NH_3 was computed using

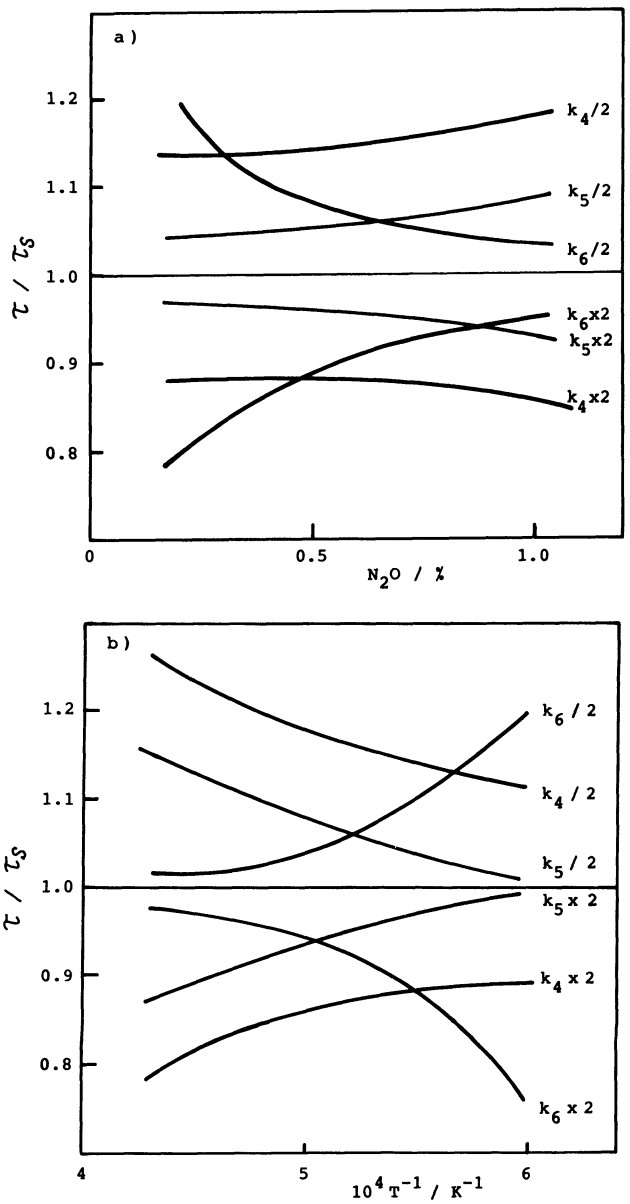

Fig. 6. Sensitivity check of the elementary reactions of (4), (5), and (6) for NH_3 consumption in NH_3–N_2O–Ar mixture. τ_s: Calculated reaction time obtained using the standard rate constants cited in Table 3. τ: Calculated reaction time obtained using the doubled ($k\times2$) or halved ($k/2$) value of the standard rate constant of Reaction (4), (5), or (6), and the standard values for other reactions. a) N_2O concentration dependence of τ/τ_s, NH_3=1%, T=2000 K, p=2 atm. b) Temperature dependence of τ/τ_s, NH_3: N_2O: Ar=1 : 1 : 98, p=2 atm.

Mechanism A, by either halving or doubling the standard rate constant of each elementary reaction shown in Table 3, and keeping other rate constants unchanged. The computed reaction time required for 10% consumption of NH_3, τ in Fig. 5, was found to be very sensitive to the change in the rate constants of Reactions (1) and (4)—(6), but not sensitive to those of

Table 4. Experimental Results for Mixture III

Run	T_{20} / K	p_{20} / atm	τ / μs	$k_4 \times 10^{-11}$ / $cm^3\ mol^{-1}\ s^{-1}$
31	2000	2.06	28±2	4.8±1.5
32	2060	2.14	17±2	10.0±2.0
33	2110	2.05	18±2	7.2±2.0
34	2110	2.13	15±2	9.1±2.0
35	2190	2.15	12±2	5.7±3.0
36	2260	2.09	8±2	13.0±5.0

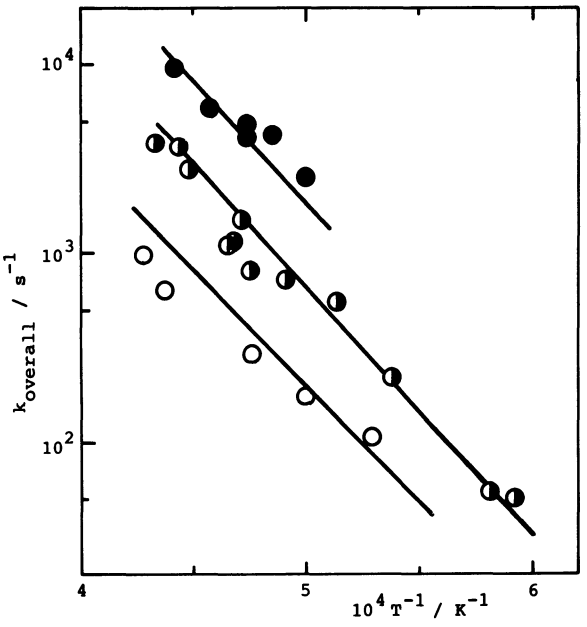

Fig. 7. Comparison of the measured overall rate constants for NH_3 (symbols) with calculated ones (lines). ○: Mixture II, ●: mixture III, ◑: mixture IV.

other elementary reactions. Examples of these results of the sensitivity checks comparing the effects by Reactions (4)—(6) are shown in Figs. 6 a) and b). From the figures, it is shown that the calculated reaction time τ is not sensitive to the rate constant of Reaction (6), when the N_2O concentration is higher than 1% (when NH_3 is 1%) and the temperature is higher than 2000 K. Therefore, mixtures I and II were omitted for the simulation to determine the value of k_4 without using reaction (6). Also, when the N_2O concentration is higher than that of NH_3, it is considered that the subsequent Reaction (12) becomes important. Therefore, N_2O rich mixtures was not examined in the present simulation to determine k_4 without using reaction (12). Based on the discussion, the mixture III was used for the simulation at first, in which only three Reactions (1), (4), and (5) were used.

The rate constant of Reaction (4) was determined by fitting the simulated τ value of NH_3 decay to the experimental one, where the rate constant k_1 determined in this experiment and k_5 of Fujii et al.[5] were

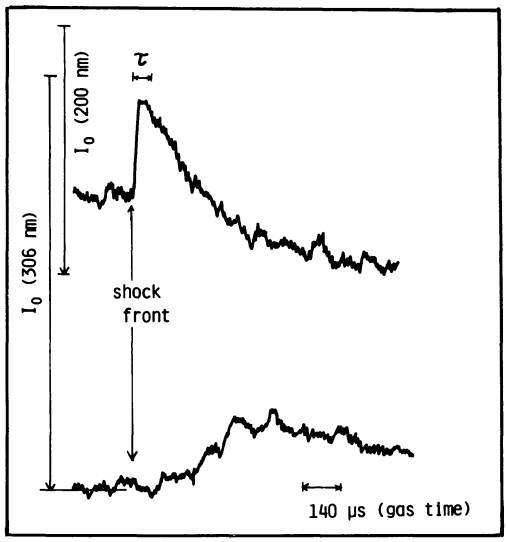

Fig. 8. Typical experimental records of NH_3 decay (upper trace) and OH formation (lower trace), NH_3: N_2O : Ar=1 : 1 : 98, T_0=1853 K, p_0=2.26 atm.

used. The rate constants of Reaction (4) obtained are shown in Table 4 and Fig. 4.

The decays of NH_3 and N_2O calculated by using reactions (1), (4), and (5) are shown by the dotted lines in Fig. 5. They agreed with the experimental values in the initial stage of the reaction. The deviation of the calculated curves from the experimental ones after the reaction time τ were improved by adding the subsequent Reactions (2), (3), and (6)—(8) to the reaction scheme, as shown by the solid lines in Fig. 5.

Computer simulatons using reactions (1)—(8) shown in Table 3 were also carried out for the mixtures II and IV, which were omitted for the simulation using reactions (1), (4), and (5) as described above. The time histories of NH_3 concentration obtained by the simulation almost agreed with the experimental ones, as well as in the case of III shown in Fig. 5. The overall rate constant for the first order decay of NH_3 was obtained according to the following equation;

$$-d[NH_3]/dt = k_{overall}[NH_3] \quad (3)$$

The comparison of the overall first order rate constant obtained by the simulation using Mechanism A with those obtained by the experiments are shown in Fig. 7.

From the results of the present study, it was found that the high temperature reaction of NH_3 with N_2O can be explained by the Reactions (1)—(8) shown in Table 3.

Formation of OH: The formation of OH were measured simultaneously with the decay of NH_3 in shock heated NH_3-N_2O equimolar mixtures. Typical experimental records of NH_3 and OH are shown in Fig. 8. Since the detection limit of OH absorption was about 5×10^{-10} mol cm^{-3}, high noise level prevented to

Table 5. Experimental Results of NH_3 Consumption and OH Formation for Mixture V

Run	T_{20} / K	p_{20} / atm	$\tau^{a)}$ / μs	$[OH]_{t=100}$ / mol cm^{-3}
51	1770	2.00	78±5	4.0×10^{-10}
52	1802	1.92	110±5	4.6
53	1841	2.10	84±5	8.0
54	1854	2.02	62±5	7.8
55	1876	2.14	54±5	8.3
56	1883	2.06	70±5	8.8
57	1953	2.00	42±5	8.2
58	1956	1.99	39±5	9.1
59	1953	2.02	38±5	1.1×10^{-9}
60	1990	2.00	28±5	2.0
61	2040	2.12	25±5	2.8

a) τ for 10% consumption of NH_3.

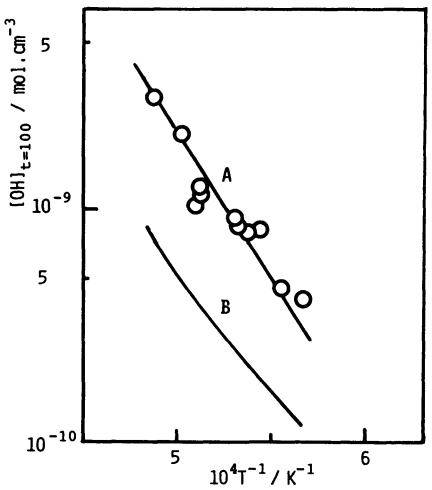

Fig. 9. Comparison of the experimental OH concentrations at $t=100$ μs (symbols) with those obtained by Mechanisms A and B (lines), $NH_3 : N_2O : Ar = 1 : 1 : 98$.

examine the OH formation in the very initial stage of the reaction. In order to evaluate the rate of OH formation, concentration of OH at $t=100$ μs, $[OH]_{t=100}$, were taken from the experimental record of OH. The value is shown in Table 5, together with τ value of NH_3 consumption.

In order to examine the rate constants of Reactions (4) and (5), calculations were performed using the above described two mechanisms A and B. A comparison of the experimental concentrations of OH at $t=100$ μs with calculated values are shown in Fig. 9. In this figure, the values calculated by Mechanism A agree well with the experiments, but those by Mechanism B are much lower than the experiments. Also, the changes of the computed concentrations of NH_3 and OH were compared with the experiments in the period of about 50% NH_3 consumption. Figures. 10 (I) and (II) show examples of comparison of the

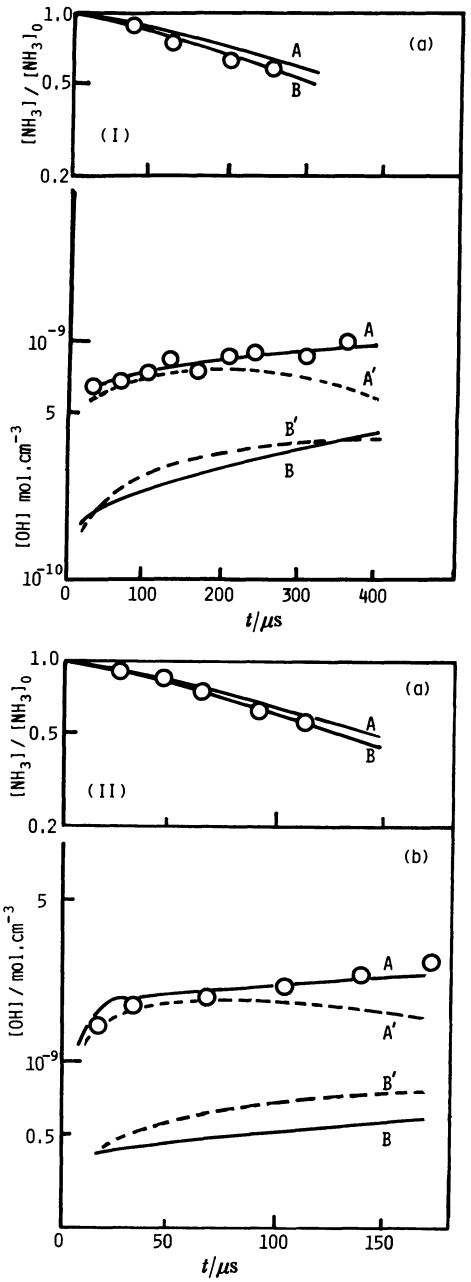

Fig. 10. Comparison of the experimental profiles (symbols) of (a) NH_3 (b) OH with those obtained by calculations (lines). Solid lines A and B are those calculated by Mechanisms A and B respectively. Broken lines A′ and B′ are those calculated by Mechanisms A′ and B′, respectively.
(I) $NH_3 : N_2O : Ar = 1 : 1 : 98$, $T_0=1854$ K; $p_0=2.25$ atm, (II) $T_0=1990$ K; $p_0=2.08$ atm.

experimental profiles of NH_3 and OH with calculated ones. As shown in the figures, consumption of NH_3 calculated by Mechanism B are faster than those by Mechanism A, however both values are not very different from the experimental values. For those of OH formation, the profiles calculated by Mechanism A are much closer to the experimental profiles than those by Mechanism B as shown in the figures.

In addition, a calculation based on Mechanism A using the k_4 and k_5 values reported by Salimian et al.[7] and a calculation based on Mechanism B using the k_4 and k_5 values reported by Fujii et al.[5,6] were carried out. The former results were not very different from the results of the calculation based on Mechanism B listed in Table 3, while the latter results were similar to those of Mechnism A listed in Table 3, in the initial stage of the reaction.

The effects of the subsequent reactions on NH_3 consumption and OH formation were also calculated. As the subsequent reactions of Mechanism A, 54 reactions from the report by Salimian et al. (Mechanism B′)[4] were adopted. The results of the calculation using 62 reactions and their reverse reactions (Mechanism A′) were compared with the experiments. Examples of the calculated profiles of NH_3 consumption and OH formation by Mechanisms A′ and B′ are shown by broken lines A′ and B′ in Figs. 10 (I) and (II). They do not deviate appreciably from the original profiles A and B, respectively, in the initial stage of the reaction, inspite of including many reactions of which rate constants are not known accurately.

From the comparisons described above, it was found that the calculated OH profiles by Mechanism A are much closer to the experiments than those by Mechanism B, and the effects of the subsequent reactions on OH formation can be ignored in the initial stage of the reaction. Thus, the rate constans k_4 and k_5 determined from Mechanism A in the initial stage of the reaction are reasonable and those obtained by Salimian et al.[7] seem to have been overestimated.

It was reported that the amount of adsorbed NH_3 on the wall of stainless steel was several times the value calculated by assuming monomolecular layer adsorption.[19] In the experiments by Salimian et al., the concentration of NH_3 introduced into the shock tube was about 4×10^{-9} mol cm^{-3} at 300 K. In such a low concentration, the adsorption of NH_3 cannot be ignored. Since in the experiments of Jefferies et al.[18] the mixture was irradiated by a TEA CO_2 laser at 10.6 μm, there is a possibility that NH_3 molecules themselves decomposed by the laser irradiation and the decomposed products accelerate the consumption of OH. This might give higher k_5 value. Also, the curved Arrhenius plots calculated by the transition state theory were based upon the arbitrary selection of parameters.[7,9,18] From those reasons, linear expressions were preferred to the curved ones for Arrhenius plots of k_4 and k_5.

In conclusion, the linear Arrhenius expressions for the rate constants of Reactions (4) and (5) combining the values at low temperatures[5,6,16,17] are proposed as follows:

(4) $NH_3 + O \longrightarrow NH_2 + OH$

$$k_4 = 10^{12.5\pm0.4}\exp(-25.5\pm2.3\ \mathrm{kJ}/RT)\ \mathrm{cm^3\ mol^{-1}\ s^{-1}}$$

(5) $NH_3 + OH \longrightarrow NH_2 + H_2O$

$$k_5 = 10^{12.5\pm0.1}\exp(-8.4\pm0.1\ \mathrm{kJ}/RT)\ \mathrm{cm^3\ mol^{-1}\ s^{-1}}$$

This work was partially supported by a Research Grant from Tanikawa Foundation, to which the authors wish to express their thanks.

References

1) N. Fujii, H. Miyama, M. Koshi, and T. Asaba, "Eighteenth Symposium (International) on Combustion," The Combustion Institute, Pittsburgh (1981), p. 873.

2) A. M. Dean, J. E. Hardy, and R. K. Lyon, "Nineteenth Symposium (International) on Combustion," The Combustion Institute, Pittsburgh (1983), p. 97.

3) A. M. Dean, M. Chou, and D. Stern, *Int. J. Chem. Kinet.*, **16**, 633 (1984).

4) S. Salimian, R. K. Hanson, and C. H. Kruger, *Combust. Flame*, **56**, 83 (1984).

5) N. Fujii, H. Miyama, and T. Asaba, *Chem. Phys. Lett.*, **80**, 355 (1981).

6) N. Fujii, H. Sato, S. Fujimoto, and H. Miyama, *Bull. Chem. Soc. Jpn.*, **57**, 277 (1984).

7) S. Salimian, R. K. Hanson, and C. H. Kruger, *Int. J. Chem. Kinet.*, **16**, 725 (1984).

8) R. K. Hanson and S. Salimian, "Combustion Chemistry," ed by W. C. Gardiner, Jr., Springer Verlag (1984), p. 361.

9) M. F. Zabielski and D. J. Seery, *Int. J. Chem. Kinet.*, **17**, 1191 (1985).

10) D. L. Baulch, D. D. Drysdale, D. G. Horne, and A. C. Lloyd, "Evaluated Kinetic Data for High Temperature reactions," Butterworths, London (1973), Vol. 2.

11) T. Just, "Shock waves in Chemistry," ed by A. Lifshitz, Marcel Dekker, Inc., New York (1981), p. 279.

12) N. Fujii, M. Koshi. H. Ando, and T. Asaba. *Int. J. Chem. Kinet.*, **11**, 285 (1979).

13) W. C. Gardiner, Jr., B. F. Walker, and C. B. Wakefield, "Shock Waves in Chemistry," ed by A. Lifshitz, Marcel Dekker, Inc., New York (1981), p. 319.

14) K. Saito and J. N. Bradley, unpublished data.

15) K. Kirchner, N. Merget, and C. Schmidt, *Chem. Ing. Tech.*, **46**, 661 (1974).

16) R. A. Perry, *Chem. Phys. Lett.*, **106**, 223 (1984).

17) R. D. Stephens, *J. Phys. Chem.*, **88**, 3308 (1984).

18) J. B. Jeffries and G. P. Smith, *J. Phys. Chem.*, **90**, 487 (1986).

19) M. Yumura, T. Asaba, Y. Matsumoto, and H. Matsui, Int. *J. Chem. Kinet.*, **12**, 439 (1980).